Title

Encapsulation and Characterization of Proton-Bound Amine Homodimers in a Water Soluble, Self-Assembled Supramolecular Host

Authors

Pluth, Michael
Fiedler, Dorothea
Mugridge, Jeffrey
et al.

Publication Date

2009-01-31

Title:

Encapsulation and Characterization of Proton-Bound Amine Homodimers in a Water Soluble, Self-Assembled Supramolecular Host

Author Affiliations:

Michael D. Pluth, Dorothea Fiedler, Jeffrey S. Mugridge, Robert G. Bergman, Kenneth N. Raymond

Department of Chemistry, University of California, Berkeley, California, 94720-1460, USA

Division of Chemical Sciences, Lawrence Berkeley National Laboratory, Berkeley, California, 94720, USA

Corresponding Authors:

Prof. Robert G. Bergman, Prof. Kenneth N. Raymond

Department of Chemistry, University of California, Berkeley, CA 94720-1460 (USA). Fax: (+1) 510-642-7714 (Bergman). Fax: (+1) 510-486-5283 (Raymond).

E-mail: rbergman@berkeley.edu, raymond@socrates.berkeley.edu

Manuscript Information:

23 Pages, 8 Figures, 3 Tables

Author Contributions:

MDP, DF, JSM, RGB and KNR designed the research, MDP, DF, JSM performed the research, MDP, RGB, and KNR analyzed the data, MDP, RGB, and KNR wrote the paper. The authors declare no conflicts of interest.

Abstract:

Cyclic amines can be encapsulated in a water-soluble self-assembled supramolecular host upon protonation. The hydrogen bonding ability of the cyclic amines, as well as the reduced degrees of rotational freedom, allows for the formation of proton-bound homodimers inside of the assembly which are otherwise not observable in aqueous

solution. The generality of homodimer formation was explored with small *N*-alkyl aziridines, azetidines, pyrrolidines and piperidines. Proton-bound homodimer formation is observed for *N*-alkylaziridines (R = methyl, isopropyl, tert-butyl), *N*-alkylazetidines (R = isopropyl, tertbutyl), and *N*-methylpyrrolidine. At high concentration, formation of a proton-bound homotrimer is observed in the case of *N*-methylaziridine. The homodimers stay intact inside the assembly over a large concentration range, thereby suggesting cooperative encapsulation. Both G3(MP2)B3 and G3B3 calculations of the proton-bound homodimers were used to investigate the enthalpy of the hydrogen bond in the proton-bound homodimers and suggest that the enthalpic gain upon formation of the proton-bound homodimers may drive guest encapsulation.

Introduction

Hydrogen bonding and protonation play vital roles in both chemical and biological phenomena as one of the most prevalent intermolecular forces in nature.(1-4) Although hydrogen bonding is often viewed as a weak interaction, the strength of a special class of strong hydrogen bonds, often referred to as ionic hydrogen bonds, can range from 5 to 35 kcal/mol.(5) These strong hydrogen bonds are important in nucleation, self-assembly, protein folding, reactivity of enzyme active sites, formation of membranes in biological systems and biomolecular recognition.(5-7) Due to the importance of hydrogen bonding in so many aspects of chemical and biological systems, a number of synthetic and theoretical studies have examined their magnitude and origin.(8, 9) Many of the computational studies have focused on simple proton-bound homodimers and heterodimers, where two neutral bases are bound by one proton (Figure

1), since experimental energies for these complexes can be obtained from gas phase thermochemical studies such as variable temperature high pressure mass spectrometry.(5)

In simple hydrogen-bonded complexes such as those shown in Figure 1, the hydrogen bond strength is maximized when the proton donor and proton acceptor have similar proton affinities. Therefore, the strongest hydrogen bonds are formed when the donor and acceptor molecules are identical.(5) Although the proton-bound homodimers and heterodimers can be observed in the gas phase, solution studies of these types of complexes remain rare. To the best of our knowledge, there are no examples of the formation (or observation) of proton-bound homodimers or heterodimers in hydrogen-bonding solvents, but rather only in aprotic organic solvents.(5, 10)

Previous work in the Raymond group has explored the formation, guest exchange dynamics, and mediated reactivity of the self-assembled supramolecular host molecule $[Ga_4L_6]^{12-}$ (**1**, L = *N,N′-bis*(2,3-dihydroxybenzoyl)-1,5-diaminonaphthalene) (Figure 2).(11-14) The water-soluble **1** maintains a hydrophobic interior cavity, ranging from approximately 250 – 430 $Å^3$ depending on the encapsulated guest,(15) which is isolated from bulk solution. Although both monocationic and neutral guests are encapsulated in aqueous solution,(16) we have previously shown that monocations are preferentially encapsulated. In our exploration of encapsulated protonated guests, we have shown that protonation can allow for encapsulation of amine guests and have also shown that chelating amines are able to intramolecularly share one proton to allow for observation of the nitrogen inversion bond rotation process (NIR) inside of the assembly.(17) We have used the thermodyanic stabilization of protonated guests in **1** to demonstrate that acid-catalyzed hydrolyses of acetals and orthoformates can be carried out in basic solution

inside of **1**.(18-21) Herein, we expand on the ability of **1** to encapsulate protonated substrates in the simultaneous encapsulation of multiple cyclic amines as proton bound homodimers, and in one case, a homotrimer.

Results and Discussion

Following our previous observations that chelating amines are able to intramolecularly bind a proton when encapsulated in **1**, we surmised that two separate amines may be able to simultaneously coordinate to one proton in **1**. Furthermore, synthetic host molecules have been shown to stabilize proton-bound amines, such as $N_2H_7^+$, in the solid state.(22) In order to test this hypothesis, a number of cyclic amines were investigated as potential guests because of their strong hydrogen bonding ability.(23) Furthermore, the reduced rotational degrees of freedom in the cyclic amines should attenuate the entropic penalty for simultaneously encapsulating multiple guest molecules and may allow for simultaneous encapsulation of multiple guests. For example, in the study of encapsulated neutral guests in **1**, we have observed that multiple substituted arenes with minimal degrees of rotational freedom can be simultaneously encapsulated in **1**.(24)

When an excess of *N*-methylpyrrolidine was added to an aqueous solution of **1**, the ^{1}H NMR integration of the encapsulated guest region showed that two equivalents of the amine were encapsulated (Figure 3). When only one equivalent of *N*-methylpyrrolidine was added to **1**, half of an equivalent of **1** remained empty while the other half of an equivalent of **1** encapsulated two *N*-methylpyrrolidine molecules. Encapsulation of the second equivalent of amine also minimizes the contacts between the

polar N-H of the guest with the hydrophobic cavity of **1** while simultaneously maximizing the favorable hydrophobic interactions between host and guest. To probe the structure of the encapsulated guest, the importance of protonation was investigated. Since neutral guests are only encapsulated in **1** in aqueous solution,(16) the encapsulation of *N*-methylpyrrolidine was investigated in both d_4-MeOD and d_6-DMSO to eliminate the possibility that the neutral amines were being encapsulated. The host-guest complex containing two equivalents *N*-methylpyrrolidine was cleanly formed in both d_4-MeOD and d_6-DMSO, thereby eliminating the possibility of neutral substrate encapsulation.

To understand the structure of the encapsulated species, variable temperature ^{1}H NMR experiments were performed with the intention of freezing out one conformation of the encapsulated complex. However, experiments ranging from 0 – 80 °C in water and from -60 – 50 °C in methanol did not change the ^{1}H NMR spectrum of the encapsulated guest. A likely explanation for the invariant ^{1}H NMR spectrum is that the structure of any of the conformations of the encapsulated proton-bound homodimer is C_2 symmetric. For example, the two extreme rotational conformations of the proton-bound homodimer have C_{2v} and C_{2h} symmetries respectively, but encapsulation in the *T*-symmetric host reduces the effective symmetry of both conformations to C_2 (See Supporting Information, Figure S1).(25)

Expanding the Homodimer Scope Following the observation of encapsulation of two equivalents of *N*-methylpyrrolidine, we sought to determine whether the simultaneous encapsulation was independent or cooperative. To address this question, the concentration of *N*-methylpyrrolidine and **1** was varied by the same factor from 22 mM to

0.50 mM. If the encapsulation of each molecule of *N*-methylpyrrolidine is independent, then new ^{1}H NMR resonances corresponding to the encapsulated protonated monomer should appear as the concentration of the solution is lowered. However, if encapsulation of the two molecules of *N*-methylpyrrolidine is strongly cooperative, then the ^{1}H NMR resonances of the encapsulated complex should not change during the course of the dilution experiment. In the dilution experiment, the observed ^{1}H NMR resonances at each concentration are identical, suggesting that encapsulation of both molecules of *N*-methylpyrrolidine is cooperative (Figure 4).

In order to test the generality of simultaneous encapsulation of multiple guests in **1**, a variety of *N*-alkyl aziridines (**2-5**), azetidines (**6-10**), pyrrolidines (**11-14**), and piperidines (**15-18**) were prepared and screened as potential guests in **1** (Figure 5). Although the toxicity and difficulty of preparation of low-molecular weight aziridines and azetidines have previously limited the number of synthetic studies, both synthetic and computational efforts have investigated the hydrogen bonding ability of these cyclic amines. Based on infrared studies of the *N*-methyl derivatives of the cyclic amines, it has been shown that the hydrogen-bonding ability of these complexes parallels the basicity with **2** << **14** < **6** < **10**.(23)

In screening the encapsulation of the cyclic amines shown in Figure 5, five equivalents of the desired amine were added to a 20 mM solution of **1** in D_2O.(26) Under these conditions, two equivalents of *N*-methylaziridine (**2**) were observed to be encapsulated. However, when more than fifty equivalents of **2** were added to **1**, three equivalents of **2** were found to be encapsulated. Although the ^{1}H NMR spectrum of *N*-ethylaziridine (**3**) indicated only monomeric guest encapsulation, the ^{1}H NMR spectrum

was broad, suggesting either fast guest exchange or interconversion of different conformations of the guest on the NMR timescale. Increasing the concentration of either **1** or **3** did not result in more than a single guest being encapsulated. Variable temperature ^{1}H NMR experiments from -70 – 50 °C did not result in sharper guest resonances or a change in the number of encapsulated molecules. For the two most sterically demanding aziridines investigated, *N*-isopropylaziridine (**4**) and *N*-tertbuylaziridine (**5**), clean dimer encapsulation was observed in both cases regardless of the number of equivalents of the cyclic amine added. In the azetidine family, *N*-methylazetidine (**6**) is only encapsulated as a monomer whereas *N*-isopropylazetidine (**8**) and *N*-tertbutylazetidine (**9**) were encapsulated as dimers. (Attempts to prepare *N*-ethylazetidine (**7**) have proved unsuccessful). Attempts to encapsulate higher-order oligomers of **6** under higher concentrations of either **1** or **6** proved unsuccessful. Of the pyrrolidines investigated, only *N*-methylpyrrolidine (**10**) was encapsulated as a proton-bound homodimer and none of the other pyrrolidines formed clean host-guest complexes with **1**. Similarly, *N*-methylpiperidine (**14**) was the only pyrrolidine investigated that is encapsulated in **1** and it was encapsulated as a monomer (Figure 6). It is likely that as the *N*-alkyl substitution is increased, the size of the pyrrolidines and piperidines becomes prohibitively large for formation and encapsulation of the proton-bound homodimers in **1**.(27) For all of the host-guest complexes containing encapsulated protonated amines, encapsulation of the amines into **1** was fast and stable host-guest complexes were formed within ten seconds of addition.

Observation of a Proton-Bound Heterodimer After the investigation of encapsulation of the proton-bound homodimers, the possibility of encapsulating heterodimers was explored. Binary combinations of the cyclic amines in Figure 6 were added to a solution of **1** by adding 1, 2, 5, 10, or 20 equivalents of each amine. In all but one case, a mixture of encapsulated homodimers was observed. However, when **4** and **10** were mixed, in either equal or unequal proportions, encapsulation of a new species which did not correspond to either of the homodimers was observed (Figure 7). Based on ^{1}H NMR analysis, the new encapsulated species contained one molecule of **4** and one molecule of **10**, suggesting the formation of a proton-bound heterodimer. While the origin of this selectivity is difficult to explain, the encapsulation of the proton-bound heterodimer does highlight the ability of **1** to selectively recognize the properties of the heterodimer over either of the possible homodimers.

Computational Studies of Proton-Bound Homodimers In hopes of further understanding the driving force for proton-bound amine homodimers formation in **1**, calculations were carried out using Gaussian 03(28) to investigate both the geometry of the complex and the enthalpic strength of the hydrogen bond in the proton-bound homodimers. One potential problem with calculations of this type is that standard methods of DFT single point energy calculations often do not accurately describe hydrogen-bonded compounds.(29) In order to overcome this problem, single point energy calculations were performed using the compound G3(MP2)B3 and G3B3 methods. These two methods combine multiple levels of theory using MP4 methods for G3B3 and the less computationally demanding MP2 methods for G3(MP2)B3. Both

types of G3B3 calculations have been shown to be accurate for small molecule systems with most calculated energies being within one kcal of experimentally determined energies for simple systems.(30, 31) (For a comparison of calculated and experimental hydrogen bond enthalpies of model systems, see the Supporting Information)

All of the compounds **2-10** and **14** were optimized at the B3LYP/6-31++G(d,p) level of theory with subsequent energy calculations using the B3LYP/6-31++G(d,p), G3(MP2)B3, and G3B3 methods. The calculated proton affinities for each of the cyclic amines are shown in Table 1. Although experimental proton affinities are only known for **2** (221.6 kcal/mol), **10** (227.9 kcal/mol) and **11** (228.9 kcal/mol) they agree well with the calculated values.(32, 33)(34) From the proton affinity calculations, two main trends are observed: 1) For a given ring size, the proton affinity increases as the size of the *N*-alkyl substitution increases, and 2.) as the ring size increases the proton affinity also increases.

Having demonstrated the validity of these computational methods in accurately calculating the proton affinity of the model compounds, the enthalpy of the hydrogen bond formed between the protonated amine and a second amine molecule ($[B\cdot\cdot H\cdot\cdot B]^+$) was calculated. We have previously shown through kinetic analysis that water, in either its neutral or protonated form, can enter **1**, so the enthalpy of the hydrogen bond formed between a protonated amine and water molecule ($[B\cdot\cdot H\cdot\cdot OH_2]^+$) was also calculated (21, 35) The geometry optimized structures for the $[B\cdot\cdot H\cdot\cdot B]^+$ and $[B\cdot\cdot H\cdot\cdot OH_2]^+$ complexes are shown in Figure 8. For each calculated structure, the single point energy was calculated at the B3LYP, G3(MP2)B3, and G3B3 level of theory (Table 2). As expected, based on the difference between the proton affinity of the amines and water, the enthalpy

of the hydrogen bond formed in $[B\cdot\cdot H\cdot\cdot OH_2]^+$ complexes is lower than for the $[B\cdot\cdot H\cdot\cdot B]^+$ complexes. For the $[B\cdot\cdot H\cdot\cdot OH_2]^+$ complexes, all three levels of theory gave similar results although the B3LYP energy calculations began to deviate from the G3(MP2)B3 and G3B3 calculations as the size of the molecule increased. For the $[B\cdot\cdot H\cdot\cdot B]^+$ complexes, the B3LYP calculations greatly underestimated the enthalpy of the hydrogen bond when compared to the G3(MP2)B3 and G3B3 methods.(36)

Based on the enthalpic difference between the $[B\cdot\cdot H\cdot\cdot OH_2]^+$ and $[B\cdot\cdot H\cdot\cdot B]^+$ complexes, formation of the proton-bound homodimer is highly enthalpically favorable when compared to the formation of the water adduct may help to explain the observation of the encapsulation of proton-bound homodimers in **1** (Table 3).(37) Although we did not pursue entropy calculations of proton-bound homodimer formation in the gas phase, the interpretation of entropy for the experimental solution studies with **1** are likely more complicated. Changes in solvation entropy and enthalpy in the desolvation of the amines upon encapsulation, release from solvent from the interior of **1**, and the change in solvation of **1** when changing from an 12- to 11- complex upon guest encapsulation prohibit definitive deconvolution of the different entropic components.(38)

Conclusions

In conclusion, we have demonstrated the formation and encapsulation of hydrogen-bonded homodimers in the interior of a water-soluble supramolecular assembly. To the best of our knowledge, the systems described in this study are among the largest molecules that have been subjected to G3(MP2)B3 or G3B3 calculations to date. The calculations suggest that formation of the proton-bound amine homodimers is

highly enthalpically favorable when compared to the solvent adducts of the protonated amines.

Materials and Methods

General Procedures. All NMR spectra were obtained using an AV-500 MHz spectrometer. The temperature of all variable temperature NMR experiments was calibrated with methanol or ethylene glycol standards. All reagents were obtained from commercial suppliers and used without purification unless otherwise noted. The host assembly $K_{12}[Ga_4L_6]$ was prepared as described in the literature.(39) The *N*-alkylaziridines **2-5**,(40) *N*-alkylazetidines **6**(41) and **9**(42), *N*-alkylpyrrolidines **11-13**,(43) and *N*-alkylpiperidines **15-17**(44) were prepared as described in the literature. Due to a large number of overlapping peaks prohibiting unambiguous assignment of the ^{1}H NMR resonances, the ^{1}H NMR spectra have been included in the Supporting Information rather than being numerically tabulated.

Synthetic Procedures

***N*-isopropylaminopropanol** This procedure is modified from a method described for the preparation of □-aminoalcohols.(45) In a 5 L 3-neck flask equipped with a magnetic stir bar, nitrogen inlet and oil bubbler were added absolute ethanol (2 L), 3-amino-1-propanol (75 g, 1.0 mol) and acetone (110 mL, 1.5 mol). After stirring overnight at room temperature, the reaction mixture was cooled to 0 °C in a salt/ice bath and $NaBH_4$ (56.6 g, 1.5 mol) was added slowly under a gentle flow of nitrogen over the course of three hours keeping the temperature of the reaction mixture at 5 – 10 °C. The reaction mixture was allowed to stir at 5 °C for two hours before the careful addition of 135 mL of cold

H_2O, dilution with 1.5 L of methylene chloride and filtration of the reaction mixture. The solvents were removed by rotary evaporator and the resultant oil was extracted with ether (3 x 200 mL) and dried over $MgSO_4$. After removal of the solvents, the residual oil was distilled under reduced pressure (bp 40 °C at 2 mmHg)(46) to afford a clear liquid which solidified after standing in the collection flask (61 g, 52% yield). ^{1}H NMR (500 MHz, $CDCl_3$) □: 3.52 (t, *J* = 7.5 Hz, 2H, CH_2), 3.01 (sept, *J* = 6.5 Hz, 1H, CH), 2.61 (t, *J* = 7.5 Hz, 2H, CH_2), 2.02 (bs, 2H, NH/OH), 1.52 (pent, *J* = 7.0 Hz, 2H, CH_2), 1.03 (d, *J* = 7.5 Hz, 6H, 2 x CH_3), ^{13}C{^{1}H} NMR (125 MHz, $CDCl_3$) □: 64.2, 52.1, 42.8, 23.6, 22.1.

***N*-isopropylaminoazetidine** To a flame-dried 2 L flask was added dry ether (1.5 L) and *N*-isopropylaminopropanol (61 g, 0.52 mol). Dry HCl was bubbled through the solution which resulted in the formation and the precipitation of the HCl salt of the amine. The ammonium salt was filtered and washed with dry ether under a stream of nitrogen and the residual ether was removed overnight under vacuum. The *N*-isopropylaminopropanol HCl salt (70.5 g, 0.459 mol) was added to a 250 mL Schlenk flask under N_2. The flask was cooled to 0 °C in an ice bath and chlorosulfonic acid (46 mL, 0.69 mol) was added dropwise with an addition funnel over the course of one hour. The reaction mixture was heated to 50 °C for 1 hr, to 150 °C for 2 hrs, and then heated an additional 1 hr at 150 °C under moderate vacuum (~ 15 mmHg). The reaction mixture was cooled to room temperature and 75 mL of water was added. The resultant solution was stirred slowly for three hours until most of the solid had dissolved, cooled to 0 °C, and adjusted to pH 11 with KOH pellets. The solution was extracted with Et_2O (3 x 150 mL), and the extract was dried over magnesium sulfate. Filtration followed by removal of the solvent under vacuum and subsequent distillation of the resultant oil under atmospheric pressure (bp

117 °C)(47) yielded the desired product (2.8 g, 6% yield). ^{1}H NMR (500 MHz, $CDCl_3$) □: 3.07 (t, *J* = 8.0 Hz, 4H, 2 x CH_2), 2.17 (sept, *J* = 6.5 Hz, 1H, CH), 1.97 (pent, *J* = 7.0 Hz, 2H, CH_2), 0.83 (d, *J* = 7.5 Hz, 6H, 2 x CH_3), $^{13}C\{^{1}H\}$ NMR (125 MHz, $CDCl_3$) □: 58.6, 53.2, 19.2, 18.4.

Computational Methods All calculations were performed using the Gaussian 03 software package with the GaussView graphical user interface. Geometry optimizations and unscaled frequency calculations were carried out at the B3LYP/6-31++G(d,p) level of theory. Frequency calculations were performed on all converged structures to confirm that they corresponded to local minima on their respective potential-energy surfaces. These structures and frequencies were then used as input in the G3(MP2)B3 or G3B3 zero-point corrected enthalpy calculations.

Acknowledgment. We thank Dr. Jamin Krinsky and Dr. Kathleen Durkin for assistance with calculations. This work was supported by the Director, Office of Science, Office of Advanced Scientific Computing Research, Office of Basic Energy Sciences (U.S. Department of Energy) under contract DE-AC02-05CH11231 and an NSF predoctoral fellowship to MDP and JSM.

References

1. Bachovchin, WW (2001) Contributions of NMR Spectroscopy to the Study of Hydrogen Bonds in Serine Protease Active Sites. *Mag. Res. Chem.* 39: S199-S213.
2. Frey, PA (2001) Strong Hydrogen Bonding in Molecules and Enzymatic Complexes. *Mag. Res. Chem.* 39: S190-S198.
3. Nadassy, K, Wodak, SJ, Janin, J (1999) Structural Features of Protein-Nucleic Acid Recognition Sites. *Biochem.* 38: 1999-2017
4. Wiest, O, Houk, KN (1995) Stabilization of the Transition State of the Chorismate-Prephenate Rearrangement: An ab-Initio Study of Enzyme and Antibody Catalysis. *J. Am. Chem. Soc.* 117: 11628-11639.

5. Mautner, M (2005) The Ionic Hydrogen Bond. *Chem. Rev.* 105: 213-284.
6. Chang, CJ, Chang, MCY, Damrauer, NH, Nocera, DG (2004) Proton-Coupled Electron Transfer. A Unifying Mechanism for Biological Charge Transport, Amino Acid Radical Initiation and Propagation, and Bond Making/Breaking Reactions of Water and Oxygen. *Biochim. Biophys. Acta: Bioenerg.* 1655: 13-28.
7. Kearley, GJ, Fillaux, F, Baron, M-H, Bennington, S, Tomkinson, J (1994) A New Look at Proton Transfer Dynamics Along the Hydrogen Bonds in Amides and Peptides. *Science* 264: 1285-1289.
8. Jeffrey, GA (1997) *An Introduction to Hydrogen Bonding* (Oxford University Press, New York).
9. Scheiner, S (1997) *Hydrogen Bonding. A Theoretical Perspective* (Oxford University Press, New York).
10. Graton, J, Berthelot, M, Besseau, F, Laurence, C (2005) An Enthalpic Scale of Hydrogen-Bond Basicity. 3. Ammonia, Primary, Secondary, and Tertiary Amines. *J. Org. Chem.* 70: 7892-7901.
11. Caulder, DL, Raymond, KN (1999) Supermolecules by Design. *Acc. Chem. Res.* 32: 975-982.
12. Davis, AV, Fiedler, D, Seeber, G, Zahl, A, van Eldik, R, Raymond, KN (2006) Guest Exchange Dynamics in an M4L6 Tetrahedral Host. *J. Am. Chem. Soc.* 128: 1324-1333.
13. Davis, AV, Raymond, KN (2005) The Big Squeeze: Guest Exchange in an M4L6 Supramolecular Host. *J. Am. Chem. Soc.* 127: 7912-7919.
14. Fiedler, D, Leung, DH, Bergman, RG, Raymond, KN (2005) Selective Molecular Recognition, C-H Bond Activation, and Catalysis in Nanoscale Reaction Vessels. *Acc. Chem. Res.* 38: 349-358.
15. Pluth, MD, Johnson, DW, Szigethy, G, Davis, AV, Teat, SJ, Oliver, AG, Bergman, RG, Raymond, KN (2008) Structural Consequences of Anionic Host-Cationic Guest Interactions in a Supramolecular Assembly. *Inorg. Chem.* ASAP article.
16. Biros, SM, Bergman, RG, Raymond, KN (2007) The Hydrophobic Effect Drives the Recognition of Hydrocarbons by an Anionic Metal-Ligand Cluster. *J. Am. Chem Soc.* 129: 12094-12095.
17. Pluth, MD, Bergman, RG, Raymond, KN (2008) Encapsulation of Protonated Diamines in a Water-Soluble, Chiral, Supramolecular Assembly Allows for Measurement of Hydrogen-Bond Breaking Followed by Nitrogen Inversion/Rotation. *J. Am. Chem. Soc.* 130: 6362–6366.
18. Pluth, MD, Bergman, RG, Raymond, KN (2007) Acid Catalysis in Basic Solution: A Supramolecular Host Promotes Orthoformate Hydrolysis. *Science* 316: 85-88.
19. Pluth, MD, Bergman, RG, Raymond, KN (2007) Catalytic Deprotection of Acetals in Basic Solution with a Self-Assembled Supramolecular "Nanozyme". *Angew. Chem. Int. Ed.* 46: 8587-8589.
20. Pluth, MD, Bergman, RG, Raymond, KN (2007) Making Amines Strong Bases: Thermodynamic Stabilization of Protonated Guests in a Highly-Charged Supramolecular Host. *J. Am. Chem. Soc.* 129: 11459-11467.

21. Pluth, MD, Bergman, RG, Raymond, KN (2008) Supramolecular Catalysis of Orthoformate Hydrolysis in Basic Solution: An Enzyme-Like Mechanism. *J. Am. Chem. Soc.* 130: 11423-11429.
22. Atwood, JL, Barbour, LJ, Jerga, A (2002) Supramolecular Stabilization of $N_2H_7^+$. *J. Am. Chem. Soc.* 124: 2122–2123.
23. Searles, S, Tamres, M, Block, F, Quarterman, LA (1956) Hydrogen Bonding and Basicity of Cyclic Imines. *J. Am. Chem. Soc.* 78: 4917-4920.
24. Hastings, CJ, Pluth, MD, Biros, SM, Bergman, RG, Raymond, KN (2008) Simultaneously Bound Guests and Chiral Recognition: A Chiral Self-Assembled Supramolecular Host Encapsulates Hydrophobic guests. *Tetrahedron* 64: 8362-8367.
25. We hoped to gain further information about the simultaneous encapsulation through use of natural abundance ^{14}N and ^{15}N NMR experiments; however, these methods were not amenable to this system. We also prepared methylphospholane, the phosphorus analog of **2**, in hopes of using ^{31}P experiments to investigation protonation. Methylphospholane, however, is not encapsulated as a proton-bound homodimer but rather is encapsulated as a protonated monomer.
26. Similar experiments in buffered solution provided equivalent results, thereby suggesting that the pH of the solution did not account for the difference in amine encapsulation.
27. Calculated the volumes of the $[B{\cdot\cdot}H{\cdot\cdot}OH_2]^+$ and $[B{\cdot\cdot}H{\cdot\cdot}B]^+$ complexes are available in the supporting information (Table S1). However, as we have previously shown that **1** is able to distort to accommodate variously sized guests, gauging the selectivity of amine encapsulation is difficult based solely on the volume of the guest.
28. Gaussian 03 Revision C.02 Frisch, MJ, *et al.* Gaussian, Inc., Wallingford CT, . (2004).
29. Pudzianowski, AT (1996) A Systematic Appraisal of Density Functional Methodologies for Hydrogen Bonding in Binary Ionic Complexes *J. Phys. Chem. A.* 100: 4781-4789.
30. Anantharaman, B, Melius, CF (2005) Bond Additivity Corrections for G3B3 and G3MP2B3 Quantum Chemistry Methods. *J. Phys. Chem. A.* 109: 1734-1747.
31. Redfern, PC, Zapol, P, Curtiss, LA, Raghavachari, K (2000) Assessment of Gaussian-3 and Density Functional Theories for Enthalpies of Formation of C_1-C_{16} Alkanes. *J. Phys. Chem. A.* 104: 5850-5854.
32. Hunter, EPL, Lias, SG (1998) Evaluated Gas-Phase Basicities and Proton Affinities of Molecules: An Update. *J. Phys. Chem. Ref. Data* 27: 413-656.
33. Ohwada, T, Hirao, H, Ogawa, A (2004) Theoretical Analysis of Lewis Basicity Based on Local Electron-Donating Ability. Origin of Basic Strength of Cyclic Amines. *J. Org. Chem.* 69: 7486-7494.
34. Experimentally determined pKa values for known N-alkyl cyclic amines calculated in this study are: 2 (7.86), 6 (10.40), 10 (10.46), and 14 (10.08).(22)
35. Pluth, MD, Bergman, RG, Raymond, KN (2008) The Acid Hydrolysis Mechanism of Acetals Catalyzed by a Supramolecular Assembly in Basic Solution. *J. Org. Chem.* In Press.

36. Some of the [B··H··B]+ calculations were omitted due to large size of the molecules and the corresponding time required for calculation.
37. We explored the possibility that formation of the proton-bound heterodimer in the case of [**4**··H··**10**]$^+$ was enthalpically driven due, however, the hydrogen bond enthalpy in the [**4**··H··**10**]$^+$ complex was calculated (G3MP2) to be 24.3 kcal/mol. This suggests that the shape of this heterodimer is preferred over either of the homodimers.
38. Leung, DH, Bergman, RG, Raymond, KN (2008) Enthalpy−Entropy Compensation Reveals Solvent Reorganization as a Driving Force for Supramolecular Encapsulation in Water. *J. Am. Chem. Soc.* 130: 2798–2805.
39. Caulder, DL, Powers, RE, Parac, TN, Raymond, KN (1998) The Self-Assembly of a Predesigned Tetrahedral M_4L_6 Supramolecular Cluster. *Angew. Chem. Int. Ed.* 37: 1840-1843.
40. Elderfield, RC, Hageman, HA (1949) The von Braun Cyanogen Bromide Reaction I. Application to Pyrrolidines and Ethyleneimines. *J. Org. Chem.* 14: 605-637.
41. Lambert, JB, Oliver, WL, Jr.; , Packard, BS (1971) Nitrogen inversion in cyclic N-chloroamines and N-methylamines. *J. Am. Chem Soc.* 93: 933-937.
42. Bottini, AT, Roberts, JD (1958) Nuclear Magnetic Resonance Spectra. Nitrogen Inversion Rates of N-Substituted Aziridines (Ethylenimines). *J. Am. Chem Soc.* 80: 5203-5208.
43. Aitken, DJ, Beaufort, V, Chalard, P, Cladiere, J-L, Dufour, M, Pereira, E (2002) Theoretical and Model Studies on the Chemoselectivity of a Grignard Reagent's Reaction with a Combined Aminonitrile–Oxazolidine System. *Tetrahedron* 58: 5933-5940.
44. Hayat, S, Atta-ur-Rahman;, Choudhary, MI, Khan, KM, Schumann, W, Bayer, E (2001) N-Alkylation of Anilines, Carboxamides and Several Nitrogen Heterocycles Using CsF–Celite/alkyl halides/CH_3CN Combination. *Tetrahedron* 57: 9951-9958.
45. Saavedra, JE (1985) Reductive Alkylation of b-alkanolamines with Carbonyl Compounds and Sodium Borohydride. *J. Org. Chem.* 50: 2271–2273.
46. Katritzky, AR, Baker, VJ, Brito-Palma, FMS (1980) Conformational Analysis of Aaturated Heterocycles. Part 100. 1-Oxa-3-azacyclohexanes. *J. Chem. Soc., Perkin Trans. 2* 11: 1739-1745.
47. Crimaldi, K, Lichter, RL (1980) Nitrogen-15 Nuclear Magnetic Resonance Spectroscopy. Natural-Abundance Nitrogen-15 Chemical Shifts of Aziridines and Azetidines *J. Org. Chem.* 45: 1277-1281.

Figures

(a) $2B + H^+ \rightleftharpoons [B\cdot\cdot H\cdot\cdot B]^+$

(b) $B + B' + H^+ \rightleftharpoons [B\cdot\cdot H\cdot\cdot B']^+$

Figure 1 Formation of proton bound homodimers (a) and heterodimers (b).

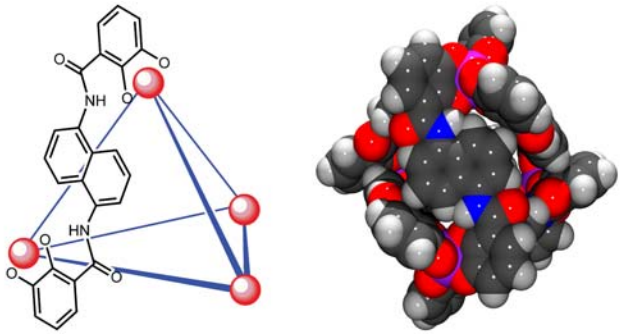

Figure 2. (Left) A schematic representation of **1** with only one ligand shown for clarity. (Right) A space-filling model of **1** as viewed down the 2-fold axis defined by the naphthalene-based ligand.

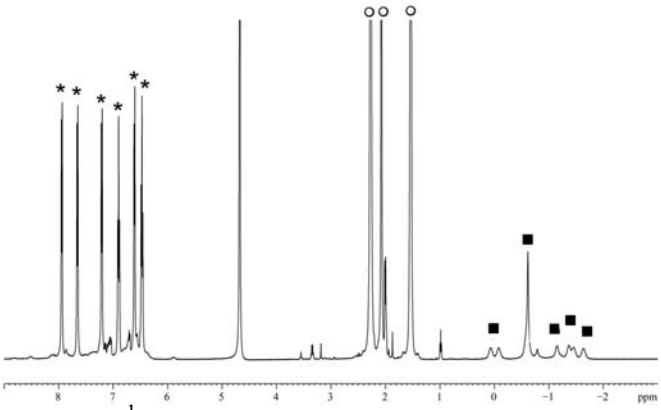

Figure 3 ^{1}H NMR spectrum of two equivalents of *N*-methylpyrrolidine encapsulated in **1** in D_2O. The resonances corresponding to the assembly (*), external *N*-methylpyrrolidine (○) and encapsulated *N*-methylpyrrolidine (■) are labeled for clarity

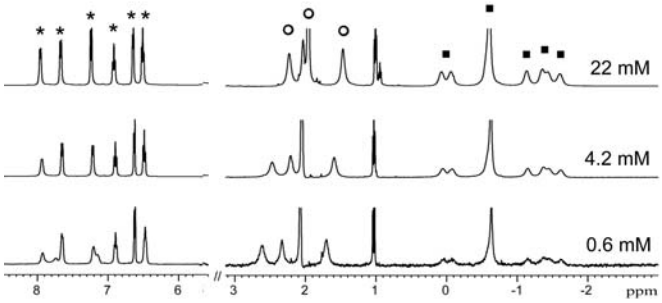

Figure 4 Dilution ^{1}H NMR experiments of *N*-methylpyrrolidine and **1**. The resonances corresponding to the assembly (*), external *N*-methylpyrrolidine (○) and encapsulated *N*-methylpyrrolidine (■) are labeled for clarity. The guest region of the spectra (3 to -3 ppm) has been enlarged 4x for clarity. The full dilution experiment is shown in Figure S2.

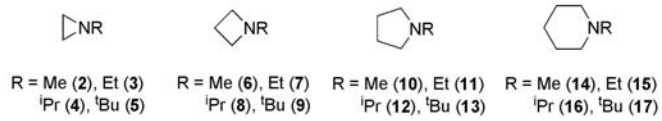

Figure 5 The scope of cyclic amines probed in **1**.

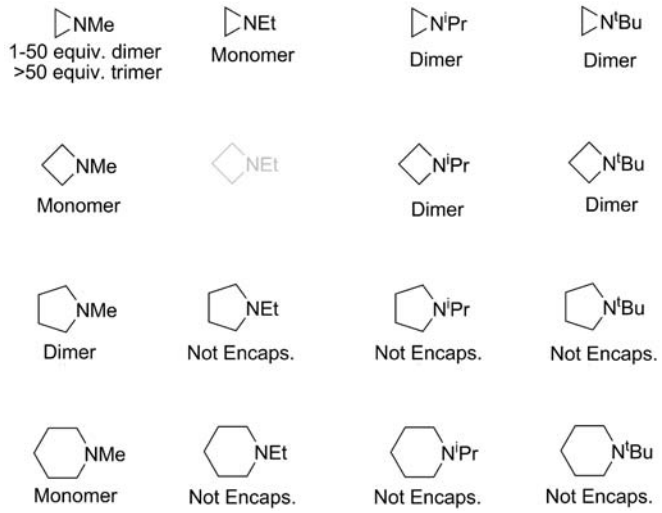

Figure 6. Scope and results of encapsulation studies in **1**.

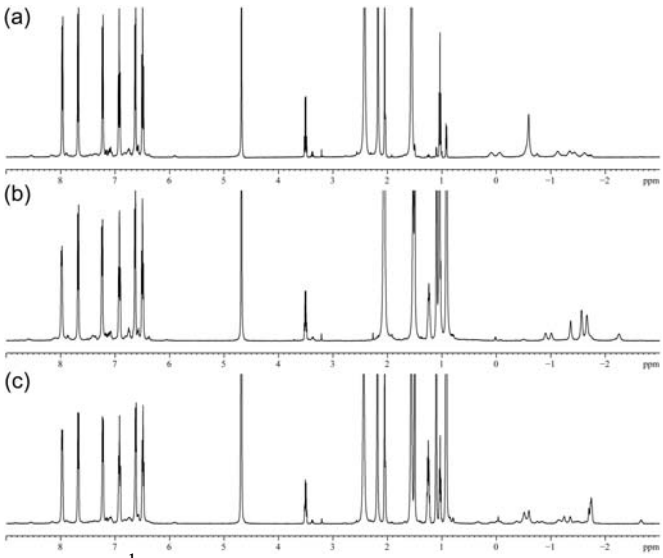

Figure 7 ^{1}H NMR spectra of a solution of **10** with **1** (a), **4** with **1** (b), and an equimolar combination of **4** and **10** with **1** (c).

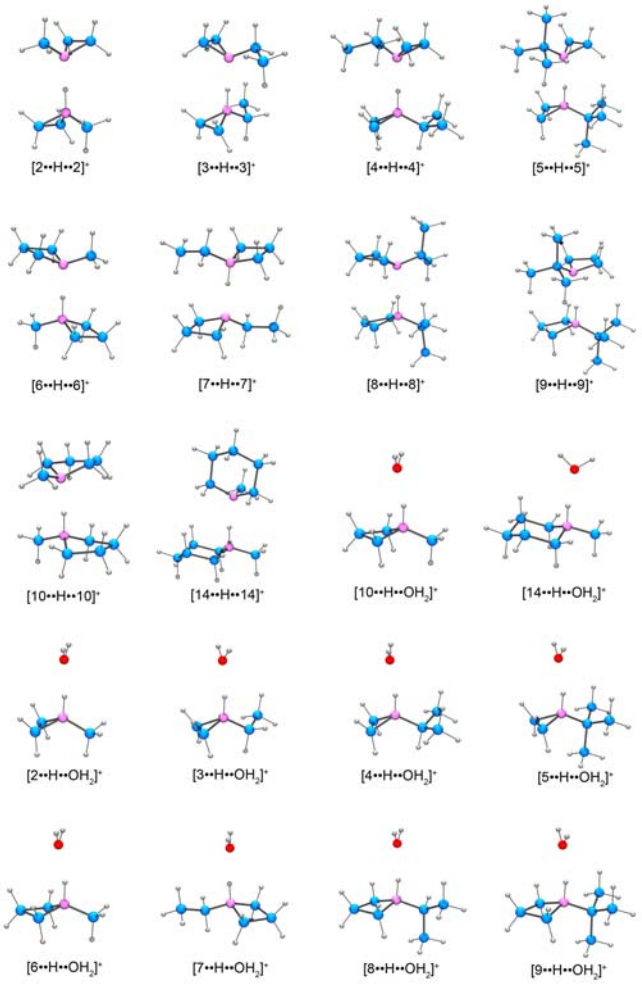

Figure 8 Calculated geometries for $[B{\cdot\cdot}H{\cdot\cdot}OH_2]^+$ and $[B{\cdot\cdot}H{\cdot\cdot}B]^+$ complexes of **2-14**. Atoms are color coded for clarity: carbon (blue), nitrogen (purple), oxygen (red), hydrogen (gray).

Tables

Table 1 Calculated proton affinities for *N*-alkyl cyclic amines.

	Proton Affinity (kcal/mol)		
Substrate	**B3LYP**	**G3MP2**	**G3**
2	222.8	221.6	221.8
3	225.2	223.9	224.0
4	227.0	225.5	224.0
5	230.3	228.8	228.9
6	228.0	227.6	227.6
7	228.3	227.8	227.7
8	232.3	231.4	231.3
9	234.6	233.8	233.7
10	229.0	228.8	228.8
14	227.8	230.6	230.3

Table 2 Calculated hydrogen bond enthalpies for the $[B\cdot\cdot H\cdot\cdot OH_2]^+$ and $[B\cdot\cdot H\cdot\cdot B]^+$ complexes.

	ΔH $[B\cdot\cdot H\cdot\cdot OH_2]^+$ (kcal/mol)			ΔH $[B\cdot\cdot H\cdot\cdot B]^+$ (kcal/mol)		
Substrate	**B3LYP**	**G3MP2**	**G3**	**B3LYP**	**G3MP2**	**G3**
2	15.8	15.4	15.9	23.1	24.9	25.5
3	14.9	14.8	15.3	21.6	25.2	25.8
4	14.2	14.4	15.0	19.5	25.2	25.7
5	13.6	14.1	14.7	17.0	24.4	---
6	14.5	14.4	15.0	20.1	24.3	24.8
7	15.8	15.9	16.4	18.7	25.1	25.4
8	11.1	11.5	12.0	11.9	19.8	---
9	12.3	13.1	13.7	11.5	21.3	---
10	13.8	14.1	14.6	17.7	24.4	24.9
14	15.9	13.6	14.0	16.5	---	---

Table 3 Comparison of the enthalpies of the hydrogen bond formation in the $[B\cdot\cdot H\cdot\cdot OH_2]^+$ and $[B\cdot\cdot H\cdot\cdot B]^+$ complexes.

	$\Delta\Delta H$[a] (kcal/mol)		
Substrate	**B3LYP**	**G3MP2**	**G3**
–2	7.3	9.5	9.6
3	6.7	10.4	10.5
4	5.2	10.8	10.7
5	3.4	10.3	---
6	5.7	9.8	9.8
7	2.9	9.2	8.9
8	0.8	8.3	---
9	-0.8	8.2	---
10	3.9	10.3	10.3
14	0.6	---	---

a: $\Delta\Delta H = \Delta H([B\cdot\cdot H\cdot\cdot B]^+) + \Delta H(H_2O) - \Delta H([B\cdot\cdot H\cdot\cdot OH_2]^+) - \Delta H(B)$